# Oxidation of Adenosine and Inosine: The Chemistry of 8-Oxo-7,8-dihydropurines, Purine Iminoquinones, and Purine Quinones as Observed by Ultrafast Spectroscopy

Denis I. Nilov, Dmitry Y. Komarov, Maxim S. Panov, Kanykey E. Karabaeva, Andrey S. Mereshchenko, Alexander N. Tarnovsky,* and R. Marshall Wilson*

Department of Chemistry and Center for Photochemical Sciences, Bowling Green State University, Bowling Green, Ohio 43403, United States

S *Supporting Information*
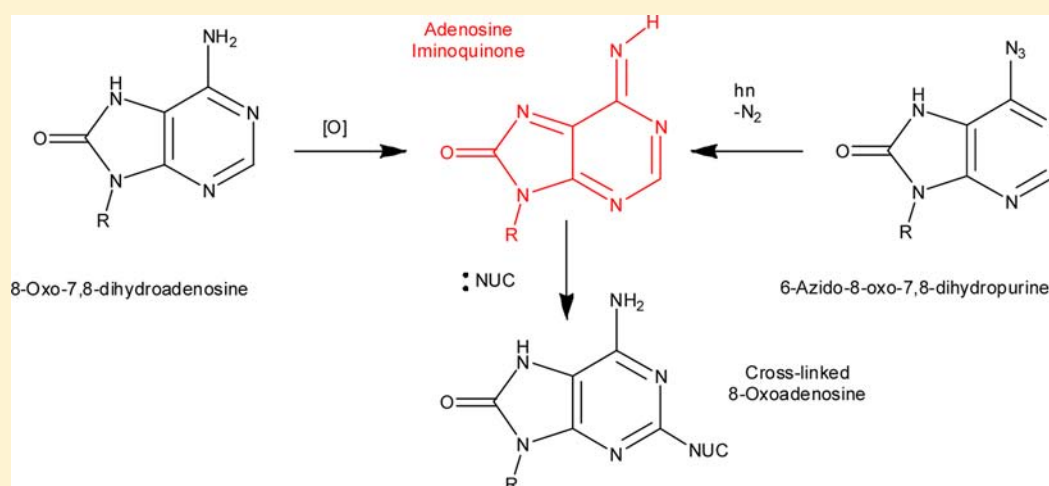
ABSTRACT: Oxidative damage to purine nucleic acid bases proceeds through quinoidal intermediates derived from their corresponding 8-oxo-7,8-dihydropurine bases. Oxidation studies of 8-oxo-7,8-dihyroadenosine and 8-oxo-7,8-dihydroinosine indicate that these quinoidal species can produce stable cross-links with a wide variety of nucleophiles in the 2-positions of the purines. An azide precursor for the adenosine iminoquinone has been synthesized and applied in ultrafast transient absorption spectroscopic studies. Thus, the adenosine iminoquinone can be observed directly, and its susceptibility to nucleophilic attack with various nucleophiles as well as the stability of the resulting cross-linked species have been evaluated. Finally, these observations indicate that this azide might be a very useful photoaffinity labeling agent, because the reactive intermediate, adenosine iminoquinone, is such a good mimic for the universal purine base adenosine.

INTRODUCTION

Oxidatively damaged nucleic acids are now widely accepted as one of the principal sources of genetic damage including possible sources of carcinogenesis, mutation, aging, and cell death.[1−8] Purines are more susceptible to single-electron oxidative damage than are pyrimidines. The oxidation potentials of unmodified bases are G (1.29 V), A (1.42 V), C (1.6 V), and T (1.7 V) versus NHE.[9] Oxidation of purine bases initially leads to 8-oxo-7,8-dihydroguanosine (8-oxoG or 8-oxodG (**1**)), 8-oxo-7,8-dihydroadenosine (8-oxoA or 8-oxodA (**2**)), and 8-oxo-7,8-dihydroinosine (8-oxoI, or 8-oxodI (**3**)), which can occur both within existing RNA/DNA strands, as well as in nucleotide pools. As indicated by the aforementioned reduction potentials, guanosine is the most easily oxidized base and has been studied in this regard extensively.[10,11] In contrast, the oxidation of adenosine and inosine has been studied much less extensively, possibly because their oxidation products are not formed in such high yields, are more difficult to detect, and because 8-oxodA (**2**) is less mutagenic than 8-oxodG (**1**).[12] These oxidized bases might lead to miscoding in DNA replication and transcription processes,[13,14] and may be associated with aging.[15] In addition, it has been noted that 8-oxo derivatives are formed more readily in RNA than in DNA, possibly because single-stranded RNA is more susceptible to oxidation than is duplex DNA or DNA protected by chromatin.[16,17]

Repair enzymes for replacing 8-oxodG (**1**) with undamaged guanosine are well-known.[1,18] The comparable repair enzymes for replacing 8-oxodA (**2**) with undamaged adenosine seem to be much less well studied possibly because 8-oxodA (2) lesions are much less mutagenic than 8-oxodG lesions, and are only

1 (8-oxoG or 8-oxodG)   2 (8-oxoA or 8-oxodA)   3 (8-oxoI or 8-oxodI)
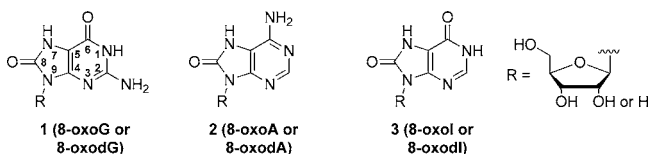
about 1/3 as common.[19−22] In fact, there seems to be less effective repair of 8-oxodA:T lesions in certain cases.[23,24] In a similar vein, the course of further oxidation of 8-oxodG (1) has been well studied and found to afford 4 and 5 (Nuc$_2$ = OH or O in water), Scheme 1.[25] Ultimately, the modified bases 4 and 5 may hydrolyze to form the urea derivative, 6. These oxidation processes are usually attributed to attack on the purine nucleus by hydroxyl radicals and other reactive oxygen species (ROS) to form the 8-oxo species 1 or 2 and their further oxidation by a variety of mechanisms.[1−8,12−14,16] However, in a separate line of research, photolysis of 8-azidoadenosine has been found to produce a diiminoquinone purine intermediate related to 7, O= replaced by HN=.[26] This intermediate is readily attacked by a variety of nucleophiles at the 2-position to form products related to 8, O= replaced by HN=. Nucleophiles examined by transient absorption spectroscopy in this work include cysteine, diethylamine, sodium hydroxide, as well as amino acid esters and nucleic acid bases. A similar quinone intermediate, 9NH$_2$, is now thought to play a pivotal role in the oxidation of 8-oxoG (1).[27−31] These observations suggest that oxidation of 8-oxopurines might follow similar oxidative pathways passing through quinoidal purines rather than via direct attack of hydroxyl radical on the purine nucleus. Thus, 8-oxoA (2) might also be susceptible to oxidative substitution to form 8 via 7, which in turn might link the oxidation of adenosine with that of guanosine, as outlined in Scheme 1, and arrive at the same final products as ROS mechanisms. Perhaps more significantly, attack on 7 by nucleophiles that do not appreciably enhance the susceptibility of 8 to further oxidation might lead to stable adducts giving rise to covalent cross-links between nucleic acids and proteins or other biomolecules. For these reasons, we have undertaken a study of adenosine oxidation using the mechanism outlined in Scheme 1 as our working hypothesis. In this study, we have concentrated on the oxidation of the 8-oxopurines 8-oxoA (2) and 8-oxoI (3), because these molecules

might form relatively stable "cross-linked" adducts at the 2-position related to 8, in contrast to the much more extensively studied 8-oxoG (1), which forms more labile "cross-linked" adducts at the 5-position as indicated in Scheme 1.[27−31]

■ RESULTS AND DISCUSSION

Chemical Oxidation Studies. Using the model for purine oxidation outlined in Scheme 1, we have investigated the oxidation of 8-oxoA (2) with a variety of oxidizing agents. The full description of the following oxidation reactions along with the spectroscopic characterization of the products is provided in the Supporting Information. Thus, treatment of 8-oxoA (2) with NBS in methanol alone at room temperature leads to formation of the methanol adduct 8OMe, R = 1′-ribosyl, Nuc$_1$ = OCH$_3$, or in a methanolic imidazole solution, the imidazole adduct 8IM, R = 1′-ribosyl, Nuc$_1$ = imidazolyl as the major products (Scheme 2). From these results, it is clear that oxidation of 8-oxoA (2) produces an intermediate that is susceptible to nucleophilic attack at the purine 2-position, and that virtually any nucleophile, even weak ones like methanol and water, vide infra, will add to the 2-position of this intermediate. We attempted to observe this reactive intermediate by conducting the oxidation reactions in the cold, but were unsuccessful. These transient studies are described in full detail in the Supporting Information. Apparently, these putative quinoidal intermediates are too reactive to survive into the second-time domain. Sigma adducts related to 10OMe have been observed previously and found to aromatize in the microsecond- and millisecond-time domains.[32]

As might be expected, oxidation of 8-oxoA (2) often produces nucleophile adducts that are very susceptible to further oxidation as outlined in Scheme 1. This subsequent oxidation is indicated by the formation of N 1′-ribosyl urea (6) observed in the NBS oxidation of 2, Scheme 2. In many cases of DNA oxidation,[14] 2′-deoxy-1′-ribosyl urea has been observed, and N 1′-ribosyl urea is occasionally observed in small amounts in the oxidations conducted in this work. It was found that the initial adducts in the 2-position are often more easily oxidized than the starting 8-oxoA (2). Thus, addition of aliphatic amines, such as diethyl amine and primary amine related to lysine, quench the intermediate 7 quite rapidly even in the cold.
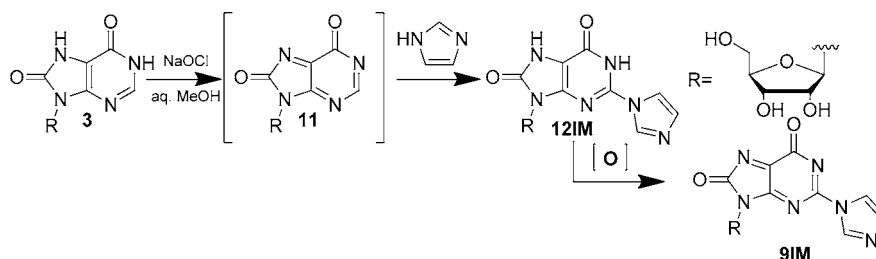
Scheme 1
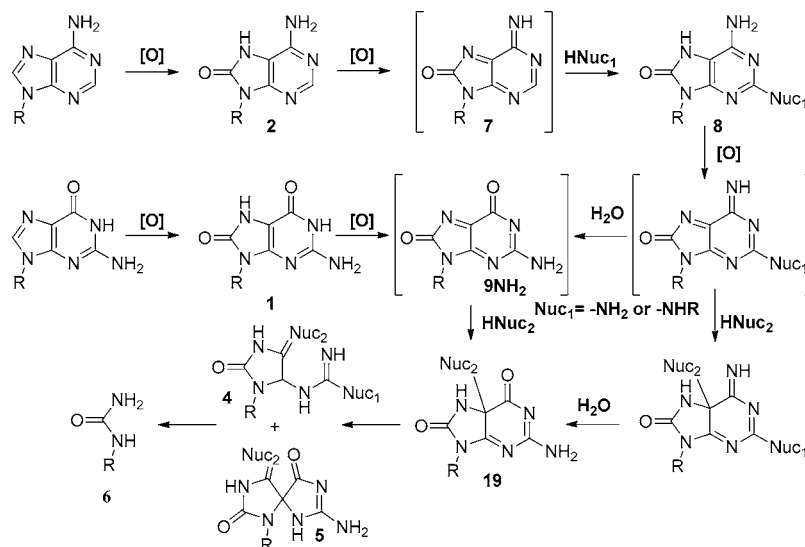
Scheme 2
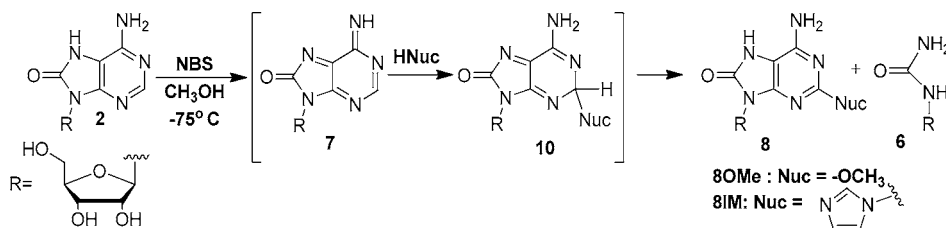
Scheme 3

Unfortunately, it has not been possible to isolate these amine adducts, possibly because they are highly susceptible to further oxidation. Related amine adducts formed in the photochemistry of 8-azidoadenosine are oxidized upon standing in air.[33] Thus, we suspect that these susceptible adducts are oxidized and destroyed more rapidly than they are formed or during the extensive HPLC procedures necessary for their isolation.

An amine that does not significantly activate the purine nucleus to further oxidation is imidazole. Thus, when the NBS oxidation of 8-oxoA (**2**) is conducted in a methanolic solution of imidazole, the imidazole adduct **8IM** (R = 1′-ribosyl, Nuc = imidazolyl) (Scheme 2) can be isolated. In many ways, imidazole is a unique amine nucleophile. The *n*-lone pair on nitrogen serves as a good nucleophile, but once attached to the purine ring, the imidazole electron pair on the nucleophilic nitrogen becomes part of the imidazole aromatic sextet, and thus is not effectively donated to the purine ring where such donation would activate the purine ring to further oxidation.

An alternative strategy for reducing overoxidation associated with the addition of electron-rich nucleophiles to the purine ring is to begin with a less electron-rich purine. The nucleic acid 8-oxoI (**3**) would seem to be an ideal candidate for testing this approach, because the electron-donating 6-amino group in adenosine has been replaced by the electron-withdrawing carbonyl group in inosine. The potential required to oxidize 8-oxoI (**3**) has been measured and found to be 1.2 V/NHE as compared to about 0.92 V/NHE for 8-oxoA (**2**),[34] and 0.74 V/NHE for 8-oxoG (**1**).[35] The relationship between these potentials is supported by the observation that treatment of 8-oxoI (**3**) with methanolic NBS, the same conditions that were successful for the oxidation of 8-oxoA (**2**), does not lead to the formation of adducts. However, treatment of **3** with the more powerful oxidizing agent sodium hypochlorite in aqueous media in the presence of imidazole leads to the formation of the imidazole adduct in the 2-position, **12IM**, Scheme 3.

Oxidative damage to nucleic acids is thought to be associated with "reactive" oxygen species (ROS) such as hydroxyl radicals and singlet oxygen.[36−41] Therefore, the visible light irradiation of both 8-oxoA (**2**) and 8-oxoI (**3**) in the presence of oxygen, imidazole, and rose bengal or riboflavin was examined in an effort to determine if singlet oxygen might affect their

transformation to **8IM** and **12IM**, respectively. These experiments produced only trace amounts of products. However, when $Na_2S_2O_8$ was added to the reactions photosensitized with riboflavin and visible light, the imidazole adducts **8IM** and **12IM** (11%) were formed, albeit in low yields. Thus, the riboflavin sensitized generation of $SO_4^{•−}$ is apparently a viable method for the oxidation of **2** and **3**. Of particular note is the observation that direct irradiation of **3** at 254 nm in the presence of $Na_2S_2O_8$ and imidazole significantly enhances the yield of **12IM**; see Table 1. In Burrows's studies of the

Table 1. Yields of Purine Oxidation Products

| purine oxidized	reaction conditions	products and % yield
2	NBS, CH_3OH	**8OMe** triacetate, 6-acetamido, 6%[a]
2	NBS, CH_3OH, imidazole	**8IM** tri-TBDMS, 19%[b]
2	NBS, H_2O, imidazole	**8IM**, 23%
2	$Na_2IrCl_6·6H_2O$, H_2O, imidazole	**8IM**, 21%
3	aq NaOCl, imidazole	**12IM**, 40.5%
3	$Na_2S_2O_8$, *hν* (254 nm), imidazole	**12IM**, 35%
3	$Na_2IrCl_6·6H_2O$, H_2O, imidazole	**12IM**, 69%

[a]Product isolated following treatment of crude reaction mixture with acetic anhydride. [b]Product isolated following treatment of crude reaction mixture with TBDMSCl.

oxidation of 8-oxoG (**1**), Na_2IrCl_6 has been found to be the oxidizing agent of choice.[42−44] This reagent proved to be one of the more effective in the oxidation of 8-oxoA (**2**) and 8-oxoI (**3**) as well; see Table 1.

While the aforementioned observations provide good circumstantial evidence for the intermediacy of the quinoidal intermediates **7** and **11**, alternative mechanistic explanations for these reactions are conceivable. Furthermore, simple oxidative methods for formation of **7** and **11** suffer from the fact that many of products that might be formed through the addition of various nucleophiles are themselves more easily oxidized than are the starting 8-oxopurines, and thus cannot be isolated or readily observed. Therefore, an alternative strategy for the

formation of iminoquinone 7 has been devised that provides much more information about the reactivity of 7 and at the same time offers the possibility of isolation of products that would be susceptible to further oxidation. Thus, the nitrene derived from 6-azido-8-oxo-7,8-dihydropurine (13) should undergo rapid, possibly solvent mediated, proton reallocation as outlined in Scheme 4 to form iminoquinone 7, and the formation and reactivity of 7 should be much more easily studied when generated under these spectroscopically favorable photochemical conditions.

Scheme 4
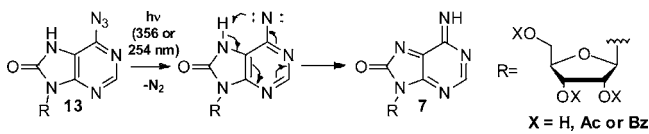
Toward this end, the triacetate and tribenzoate of azide 13, 13Ac$_3$, and 13Bz$_3$ have been synthesized[45−47] as described in detail in the Supporting Information. The preparation and irradiation of the acetylated and benzoylated derivatives greatly facilitates HPLC product analysis, but does not significantly affect the product distribution.

Irradiation of 13Ac$_3$ in methanolic solutions of imidazole affords both reduction, 2Ac$_3$, and the desired imidazole substitution product, 8IMAc$_3$, as outlined in Scheme 5. In addition, the iminoquinone hydrolysis product 3Ac$_3$ is formed as well. The imidazole adduct 8IM isolated from this azide photochemistry was compared and found to be identical to the imidazole adduct isolated from the chemical oxidation of 8-oxoA (2), Scheme 2.

Scheme 5 and Table 2 summarize the products formed in the photolyses of azides 13Ac$_3$ and 13Bz$_3$ in methanolic solutions. Because methanol by itself is a poor nucleophile, the photodecomposition of azide 13Bz$_3$ in pure methanol leads to little, if any, formation of adduct 8OMeAc$_3$. However, photolysis of methanolic solutions of 13Ac$_3$ and 13Bz$_3$ in the presence of the powerful nucleophile imidazole leads to the formation of appreciable yields of imidazole adduct 8IMAc$_3$ and 8IMBz$_3$. The formation of 3Ac$_3$ and 3Bz$_3$ is apparently due to the hydrolysis of the imino group in the iminoquinone 7Ac$_3$ and 7Bz$_3$, respectively, followed by reduction of the quinone 11 as outlined in Scheme 6.

The photochemical behavior of 8-azidoadenosine, 14, is also of considerable interest, because it is one of the most widely applied photoaffinity labeling agents used to cross-link many biological molecules. Its preparative photochemistry has been studied in detail[26] and found to proceed through the diiminoquinone 15. In this work, preparative irradiation of azide 14 was carried out at 356 nm in water in the absence of

and in the presence of imidazole (0.1 M). The analysis of these reaction mixtures indicated the formation of reduction product 16, water addition product 17OH, over oxidation product 18, dimerization products of undetermined structure, and in the presence of imidazole, imidazole adduct 17IM, Scheme 7 and Table 2.

The imidazole adducts and their acetylated and benzoylated derivatives have been obtained by several chemical and photochemical methods. In addition to the imidazole adducts 8IM and 17IM, the 8-oxoI imidazole adduct 12IM, Scheme 3, has been observed in the chemical oxidation of 8-oxoI (3). These observations, as well as similar observations for 8-oxoG,[25,27−31] are consistent with the general mechanism outlined in Scheme 1 in which the pivotal intermediates are quinoidal purines. The 8-oxoA and 8-oxoI adducts in the 2-position, 8 and 12, respectively, are distinguished from the 8-oxoG adduct in the 5-position, 19 in Scheme 1, in that the purine nuclei remain intact following nucleophile attack, and, consequently, might form stable cross-links with many other biological molecules. It should be emphasized that in these studies of quinoidal purines, 7, 11, and 21, adducts in the 5-position were not identified. In addition, the further oxidation of adducts in the 2-position, such as 8IM and 12IM, has yet to be studied in detail. The implication of the above observations with imidazole is that histidine adducts might provide relatively stable protein cross-links, but this correlation remains to be tested with the amino acid itself. While these and many related studies will be necessary to evaluate the working hypothesis outlined in Scheme 1, the availability of azide 13 has provided an ideal opportunity to probe the intermediacy of iminoquinone 7 in the early stages of this reaction scheme.

A variety of azidopurines have been used in photoaffinity labeling studies,[26] but 6-azido-8-oxo-7,8-dihydropurines (13) have never been applied in such studies. The azide 13 would seem to be the ideal tool for probing the fate/role of iminoquinone 7 in biological systems leading to gene malfunction. One might argue that the 6-azido group of 13 would alter the usual Watson−Crick hydrogen bonding or modify the normal syn/anti base conformer distribution. In addition, it is well-known that azidopyrimidines undergo azide−tetrazine tautomerization such as that shown for azide 13 in Scheme 8.[45−47] However, azide 13 displays an intense absorption at 2150 cm^{-1}. So its azide tautomer 13 is the major, if not the only, form present. Even so, both tautomers might be expected to form the nitrene precursor of 7 upon irradiation at 254 nm.[48] Thus, 13 rapidly forms the iminoquinone 7 upon irradiation (<100 ps, Scheme 4), and 7 reacts with nucleophiles so slowly (μs to ms) that there is adequate time for it to probe multiple binding sites and react with nucleophiles in the most suitable of those sites. Thus, while one might question the
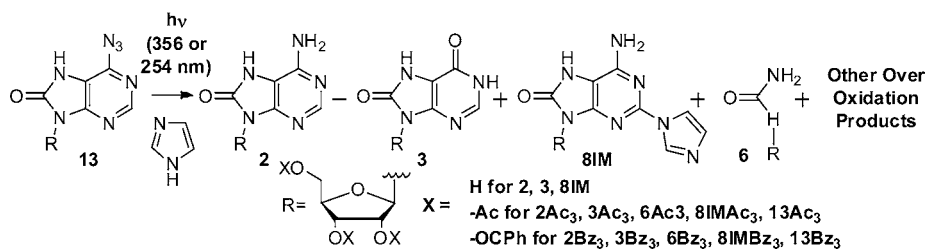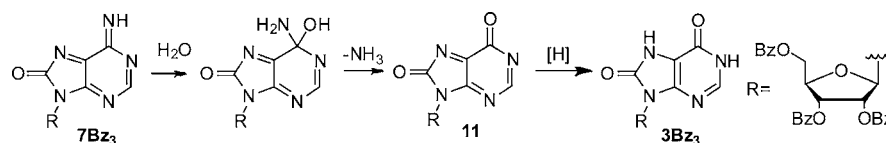
Scheme 5

Table 2. Irradiation of Azides 13Ac₃ and 13Bz₃ in MeOH and 14 in Water

azide	solvent	conditions, $h\nu = 1$ h/mmol	nuc	product distribution (%)[a]			
				2	3	8IM	unidentified[b]
13Bz₃	MeOH	254 nm 5 mmol/L	MeOH	30 Bz₃	30 Bz₃	8OMe[c]	40
13Ac₃	MeOH	254 nm 5 mmol/L	imidazole	10 Ac₃	20 Ac₃	50 Ac₃	10
13Bz₃	MeOH	356 nm 5 mmol/L	imidazole	0	30 Bz₃	50 Bz₃	20
13Ac₃	MeOH	356 nm 5 mmol/L	imidazole	20 Ac₃		60 Ac₃	20
14	H₂O 0.5% HOAc	356 nm 5 mmol/L	H₂O	16 ~7	17OH ~10	~20	18 ~20 ~20
14	H₂O 0.5% HOAc	356 nm 5 mmol/L	imidazole	16 ~20	17OH ~10	17IM ~10	18 ~20 ~20

[a] The sugar esters tend to hydrolyze partially during the course of the reaction due to the basic alcoholic conditions of the imidazole reactions. [b] These products seem to constitute a complex mixture of over oxidation or coupling products. [c] Adduct observed in only trace amounts.
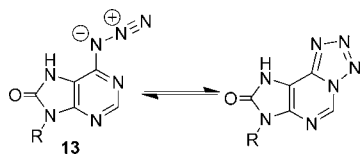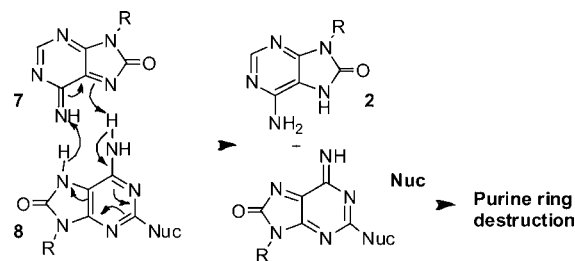
Scheme 6

Scheme 7
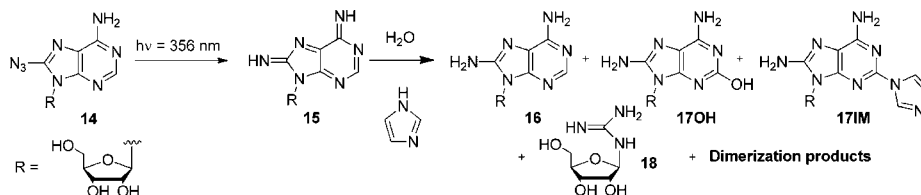
Scheme 8

viability of **13** as a mimic for the affinities of 8-oxoA (**2**), the iminoquinone **7** should be an ideal mimic for **2**.

Many 8-oxoA (**2**) and 8-oxoI (**3**) adducts are susceptible to further oxidation, which ultimately leads to the destruction of the purine nucleus, and the release of any cross-linked molecules. While such further oxidation can be minimized by the photochemical generation of the iminoquinone **7** from azide **13**, even this route suffers from adduct overoxidation possibly as outlined in Scheme 9. This problem of oxidation of cross-linked molecules requires further study and evaluation. Further oxidation of amine adducts of 8-azidoadenosine (**14**) such as the triamine **17NR₂** is a major problem, because these adducts are extremely susceptible to oxidation even by atmospheric oxygen, which leads to ephemeral cross-links and complex reaction mixtures. Therefore, further studies comparing the stabilities of the very electron-rich amine adducts such as **17NR₂** with the much less electron-rich amine adducts of **13**, see Scheme 10, would seem to be most desirable. However, at
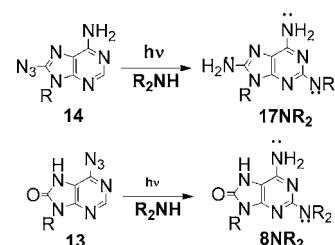
Scheme 9

this time, it would seem safe to say that **8NR₂** should be less susceptible to further oxidation than **17NR₂**.

Finally, in this section, the chemical oxidation of 8-oxo-7,8-dihydropurines has been investigated and shown to lead to

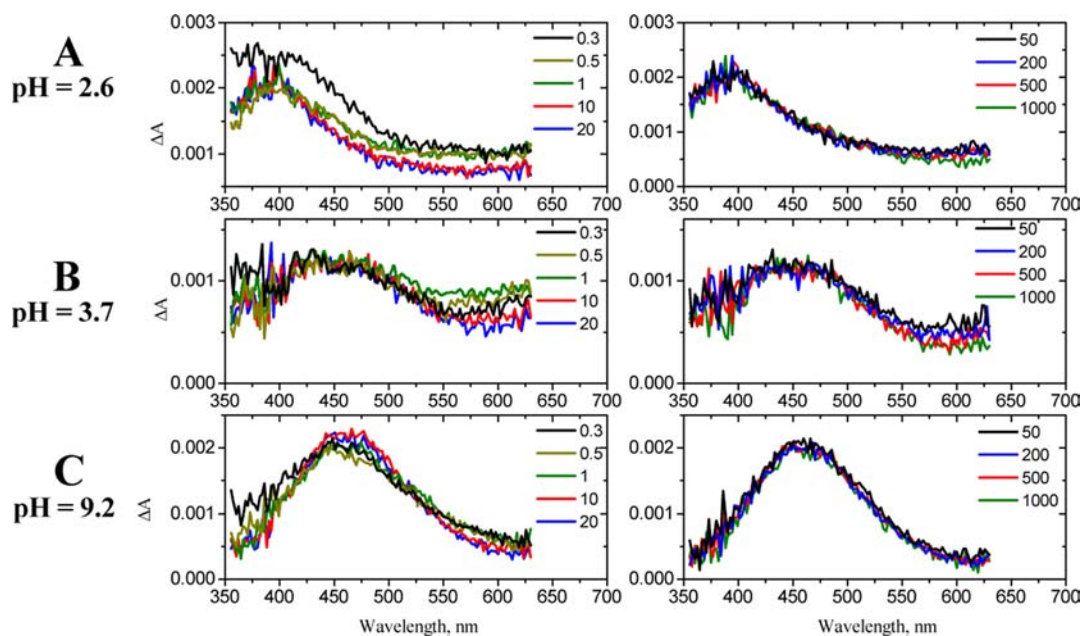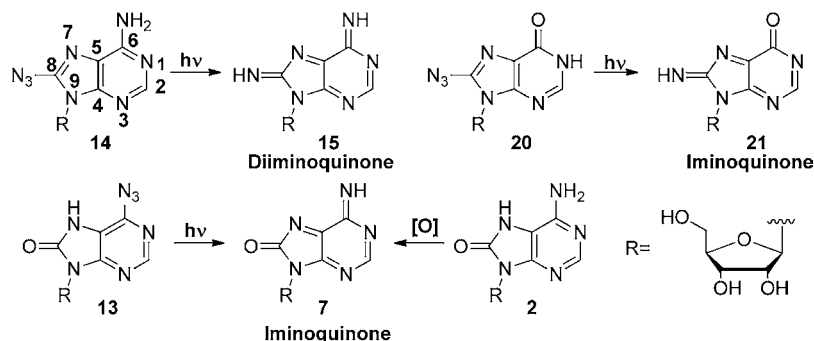**Scheme 10**

Scheme 11

Figure 1. Ultrafast transient absorption spectra of azide **14** in water solution at pH = 2.6 (A), 3.7 (B), and 9.2 (C). Time delays between pump and probe pulses are expressed in picoseconds and given in legends.
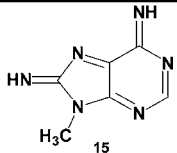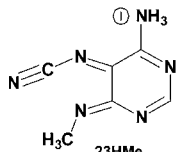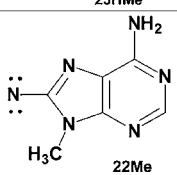
nucleophile attack and substitution at the purine 2-position. The photochemistry of 6- and 8-azidopurines leads to similar products so long as the 2-position is unsubstituted in the starting azide. Because this azide photochemistry provides an excellent tool for the spectroscopic mechanistic study of the formation of quinoidal purines and their chemistry, we have undertaken such a study and report the results in the following section.

Transient Absorption Spectroscopic Studies. Because the azide **14** provides an ideal precursor for the diiminoquinone **15** (Scheme 11),[26] the azide **13** would seem to provide an ideal precursor to the iminoquinone **7**, and the azide **20** to the iminoquinone **21**. We have studied the photochemistry of these azides in aqueous media using ultrafast transient absorption spectroscopy. The iminoquinone **7**, derived from the oxidation of 8-oxo-7,8-dihydroadenosine, **2**, and the photochemistry of the azide **13**, is probably the most interesting of these, becauase adenosine is the universal base found in DNA, RNA, and many coenzymes. However, 8-azidoadenosine, **14**, is a widely used photoaffinity labeling agent, which has been shown to be a precursor of the diiminoquinone **15** involved in the cross-linking of this reagent to many biomolecules,[49] and is included in this study to contrast its ease of formation and the reactivity with that of iminoquinones **7** and **21**.

Photodecomposition of azide **14** following 270 nm excitation has been studied previously by ultrafast transient absorption spectroscopy with a 400 fs time resolution.[26] In the current work, transient absorption, ΔA, spectra of **13**, **14**, and **20** were measured and studied following 300 nm excitation with a time resolution of 200−300 fs (limited by solvent artifact, and, as a result, solvent dependent, see Supporting Information). The transient spectra of **14** were found to be strongly pH dependent in the present work. At pH = 2.6 or lower, a band centered at λ_{max} = 390 nm develops within ca. 500 fs, spectrally narrows indicative of vibrational relaxation of the responsible product species (exponential time constants (τ) are wavelength dependent ranging between ca. 0.5−10 ps), and remains constant for at least 1 ns (Figure 1A). In contrast, at pH = 9.2 or higher, the formation of the 390 nm band was not observed in aqueous solution of azide **14**. Instead, a new band centered at λ_{max} = 465 nm develops within 300 fs, undergoes several-picosecond spectral sharpening, and then survives for at least 1 ns (Figure 1C). Transient absorption spectra of azide **14**, recorded at intermediate pH values such as pH = 3.7 (Figure 1B), have a broad band centered at λ_{max} = 440 nm. This band is broader as compared to the bands at pH = 2.6 and 9.2 and seems to be a combination of the 390 and 465 nm bands.

Scheme 12
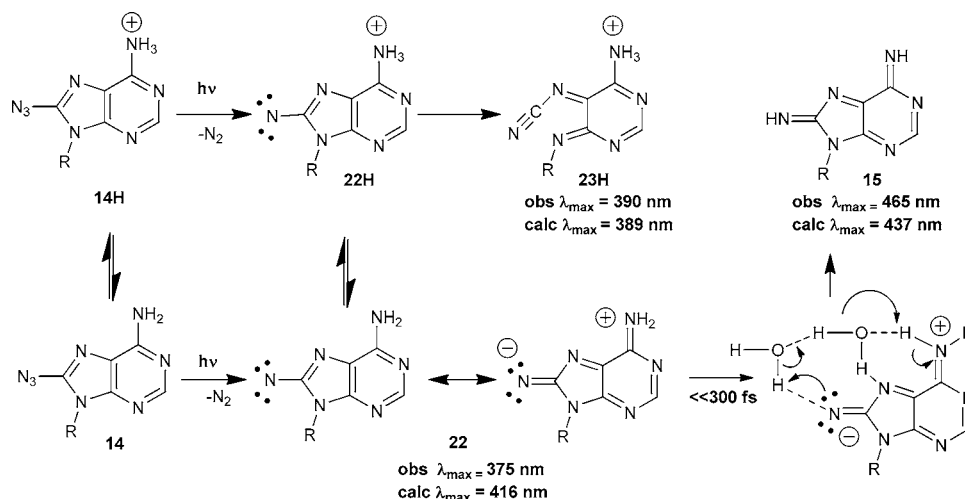
Table 3. Calculated Vertical Excitation Energies and Oscillator Strengths (*f*) for Intermediates 15Me, 23HMe, and 22Me in Methanol[a]

Species	λ (nm) experiment	λ (nm) (*f*)	
		B3LYP/6-31G(d)	CASPT2//CASSCF(14,11) /ANO-RCC
15	465	444 (0.1756)	437 (0.2625)
23HMe	390	389 (0.1887)	-
22Me Closed-shell Singlet	375	421 (0.1355)	416 (0.1060)

[a]All calculations were performed in the gas phase.

Clearly two quite different intermediates are being generated from azide **14** at different pH's. Under acidic conditions, the 6-amino group of **14** will be protonated, **14H** in Scheme 12. The nitrene **22H** will not be stabilized by the powerful electron-donating effect of the unprotonated amino group. Under these conditions, rapid opening of the five-membered ring to the iminonitrile **23H** might occur.[26,50−53] In contrast, under basic conditions, the nitrene will be stabilized by the powerful electron-donating effect of this amino group and becomes the powerful base, **22**, which will lead to proton reallocation to form **15**. The formation of **15** is complete within ca. 300 fs. The resulting vibrationally hot diiminoquinone **15** then undergoes vibrational cooling manifested by spectral narrowing over several picoseconds, Figure 1C. Spectral assignments of intermediates and products observed throughout the current work were assisted by calculating vertical excitation transitions (VETs) of these species at the TDDFT (B3LYP functional, 6-

31G(d,p) basis set) and CASPT2/ANO-RCC levels of theory.[54] The calculated absorption spectra (Scheme 12, Table 3) support the aforementioned assignments. Thus, the ring-cleaved iminonitrile **23H** is calculated to have a major electronic transition at 389 nm, Scheme 12, and this ring-opening might easily occur within 500 fs, Figure 1A. In contrast, the diiminoquinone **15** is calculated to display absorption in the 430−450 nm region.[26] The fast sub-300 fs proton reallocation necessary to transform **22** in to **15** in Scheme 12 apparently takes place via some type of proton relay mechanism, which might be a coordinated process related to that shown in Scheme 12. Calculations of energetics involved in the transformation of **22** to **15** via such a proton relay process (a relaxed reaction coordinated scan involving two water molecules) indicated rather high energy barriers on the order of 18 kcal/mol for the proton-relay process shown in Scheme 12. Therefore, if this type of proton reallocation is to take place
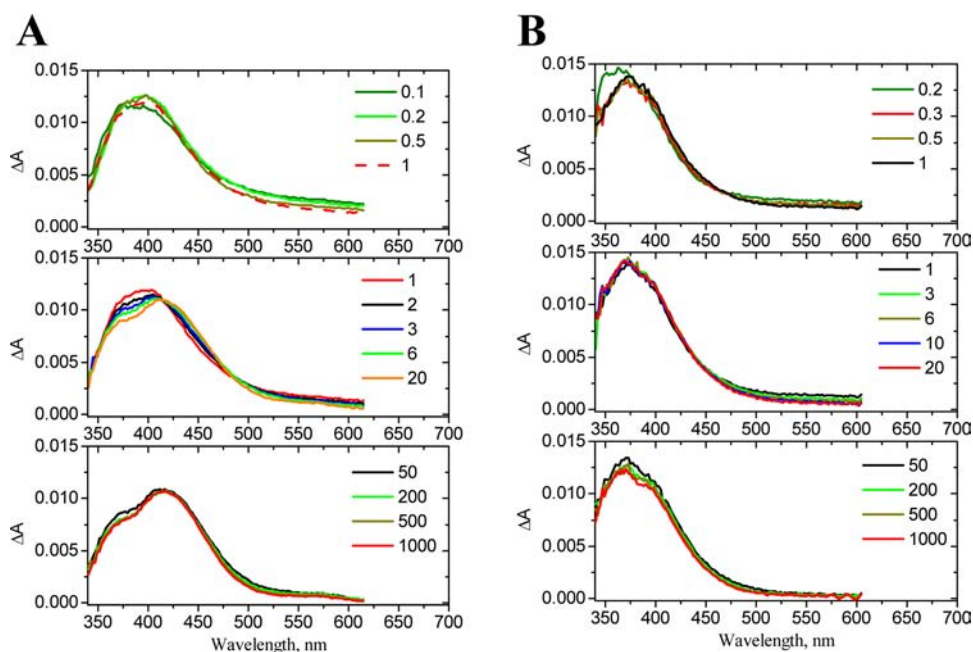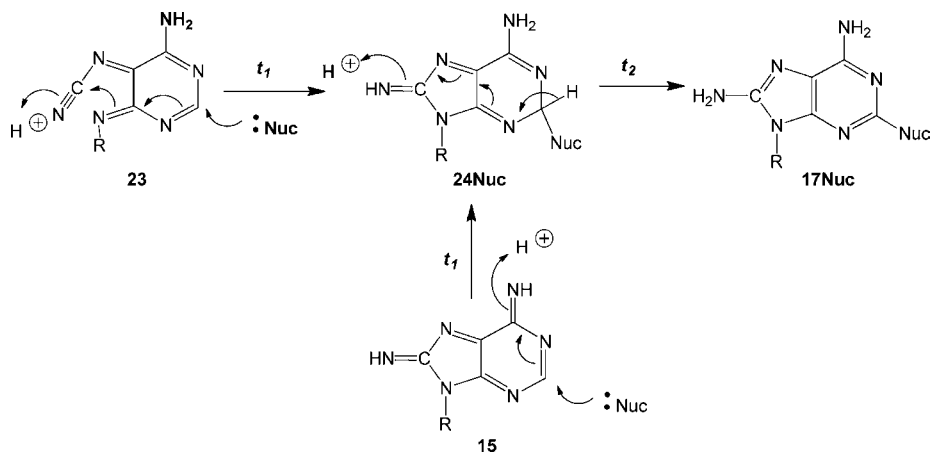
Scheme 13

Figure 2. Ultrafast transient absorption spectra of acylated derivatives of azide **14** in nonprotic solvents. Column A: **14Bz₅** (1 mM) in dichloromethane. Column B: **14Ac₅** (1 mM) in methylcyclohexane. Time delays in picoseconds between pump and probe pulses are given in the legends. The 395 and 375 nm absorption bands develop within the first 300 fs after the excitation pulse, and they decay either with formation of two absorption bands at 370 and 416 nm (τ = 2.5 ps, A) or very slowly on a several nanosecond time scale (B).

within the <300 fs window indicated, either proton tunneling will have to play a very significant role, or the energetics of the system must change appreciably upon solvation with more than two water molecules in the formation of the species absorbing at 465 nm.

Because there are apparently two alternative nitrene decay pathways, one via five-membered ring cleavage and the other via diiminoquinone formation, there must be two convergent product forming pathways, because the same products are apparently formed from both types of intermediates. Two such alternative pathways for nucleophile attack are outlined in Scheme 13. This same dichotomy has been discussed in detail in previous papers,[26,50−53] and little new can be added to that discussion except to note that these two pathways are regulated by the pH of the solution and other factors that alter the availability of electron density on the nitrene nitrogen.

One such factor is the acylation of the 6-amino group, which has an effect similar to that of the protonation of this amino

group, and leads to five-membered ring fragmentation in both **14Bz₅** and **14Ac₅**, Figure 2. Thus, excitation of **14Bz₅** in a nonprotic solvent leads to transient absorption bands at λ_{max} = 395 nm within ca. 300 fs. This band relaxes into two bands at 370 and 416 nm with τ = 2.5 ps (Figure 2A). In a similar fashion, irradiation of **14Ac₅** in a nonprotic solvent affords a band centered λ_{max} = 375 nm with τ = 1.5 ps that undergoes little or no further change (Figure 2B). These bands centered at λ_{max} = 365−375 nm are assigned to corresponding nitrenes and the mature bands in the 375−416 region to the corresponding ring-opened iminonitriles. Apparently even acyl groups on the 6-amino group are sufficiently electron withdrawing to favor the ring-opening pathway, if alternative protonation pathways are not available.

In previous work with electron-rich nitrenes, we observed that the rate of nitrene protonation/relaxation was related to the structure of the proton source with the process in methanol being ca. 4 times faster than that in 2-propanol.[32] This same
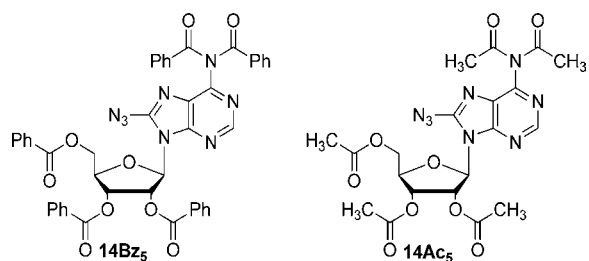
general trend is observed with azide **14**, Figure 3. Thus, in methanol, nitrene **22** (λ_{max} = 460 nm) undergoes proton reallocation/relaxation, which is characterized by an exponential rise-time constant of τ = 1.5 ps. While in 2-propanol, a significantly longer reallocation/relaxation time constant is observed, τ = 2.5 ps. Thus, proton transfer, Scheme 12, proceeds with about the same very rapid rate in water and methanol, but with a slightly slower rate in 2-propanol. In all of these systems, this proton transfer ranks among the most rapid yet observed.[55−58]

The reactions of diiminoquinone **15** with various nucleophiles were studied by nanosecond transient absorption spectroscopy (Table 4). Thus, azide **14** was irradiated in water at pH = 3.1, 6.5, and 11.5 (Figure 4), and in 0.1 M aqueous solutions of imidazole (Figure 5A), a model compound for histidine, and in 0.1 M sodium phenoxide (Figure 5B), a model compound for tyrosine. According to these spectra, quenching of diiminoquinone **15** under neutral conditions, pH = 6.5, Figure 4B, is a relatively slow process (Schemes 7, 13, and 14), with quenching of diiminoquinone **15** occurring in τ_1 = ca. 100 μs, and subsequent aromatization of the corresponding C_2-adduct proceeding with τ_2 > 35 ms. However, these processes are accelerated under both acidic and basic conditions to τ_2 = ca. 20 ms at pH = 3.1 and τ_2 = 4.2 ms at pH 11.5. The reaction of **15** with 0.1 M aqueous sodium phenoxide takes place with τ_2 = 3 ms (Figure 5B) and more rapidly with imidazole, τ_2 = 900 μs (Figure 5A). These nucleophilic substitution reactions all proceed through intermediates similar to **24Nuc** in Scheme 13. The initial

diiminioquinone **15** is only clearly visible in Figure 4B, the pH = 6.5 spectrum, λ_{max} = 450 nm at 32 μs. It is formed in the picosecond time domain and slowly reacts with nucleophiles and rearomatizes within the microsecond−millisecond time domain. It is this rearomatization process that is visible in Figure 4A and C and Figure 5A and B. It is interesting to compare the behavior of 8-azidoadenosine, **14**, with that of 8-azidoinosine, **20**. The nitrene **25** generated from **20** is not conjugated to a powerful electron-donating group, and therefore might not undergo proton reallocation to form the iminoquinone **21**, Scheme 15. Thus, irradiation of **20** in water, pH = 1.7−7.5, alcohols, or aprotic solvents such as dichloromethane all lead to the rapid development of a 380 nm band characteristic of opening of the five-membered ring and formation of the iminonitrile **26**, Scheme 15. Because no proton reallocation patterns could be observed under any conditions examined, it would seem that irradiation of **20** leads to opening of the five-membered ring to form **26** exclusively, Scheme 15. It is worthy of note that during theoretical structural optimization of nitrene **25** using either DFT or MP2 calculations, the C8−N9 bond always broke to form the iminonitrile isomer **26**. The most informative of these transient experiments was that conducted in water at pH 7.5 (Figure 6A). The very broad absorption at 450−600 nm is assigned to the nitrene **25** that decays with the same time constant as the growth of the iminonitrile **26** band at 380 nm, τ = 7 ps. In contrast, opening of the five-membered ring in methanol (Figure 6B) and dichloromethane (Figure 6C) is more rapid and apparently occurs in near-concert with nitrene formation, because there is only a slight narrowing of the 380 nm peak, which can be attributed to vibrational cooling of the open iminonitrile **26**. Furthermore, the iminonitrile **26Ac₃** displays spectroscopic behavior similar to that of the diiminoquinone **15** in the microsecond−millisecond time domains (Figures 7 and 4, respectively). Thus, both **26Ac₃** and **23H** react with water or methanol within 15−20 ms. However, it seems that the iminonitriles are better electrophiles than are the iminoquinones: iminonitrile **26Ac₃** reacts much more rapidly with
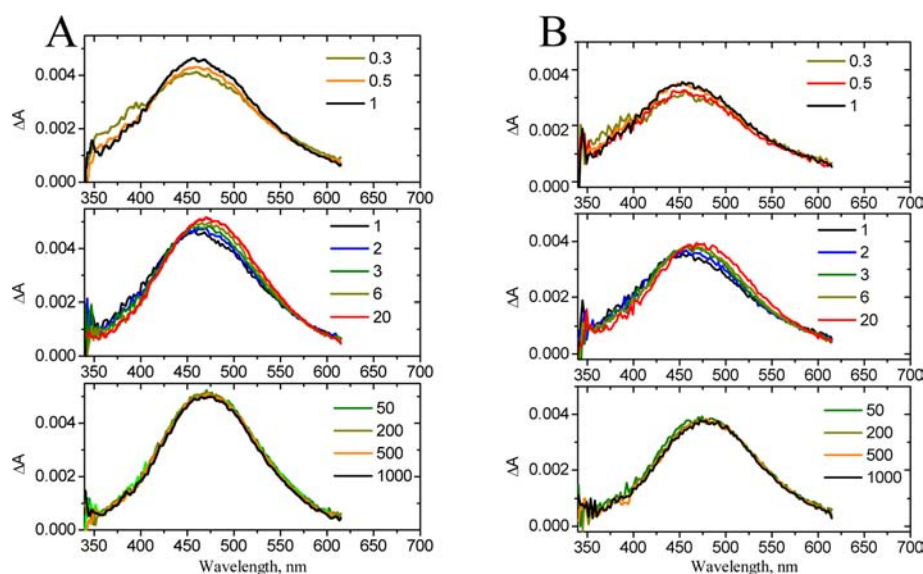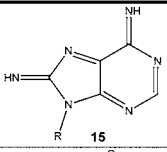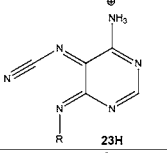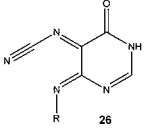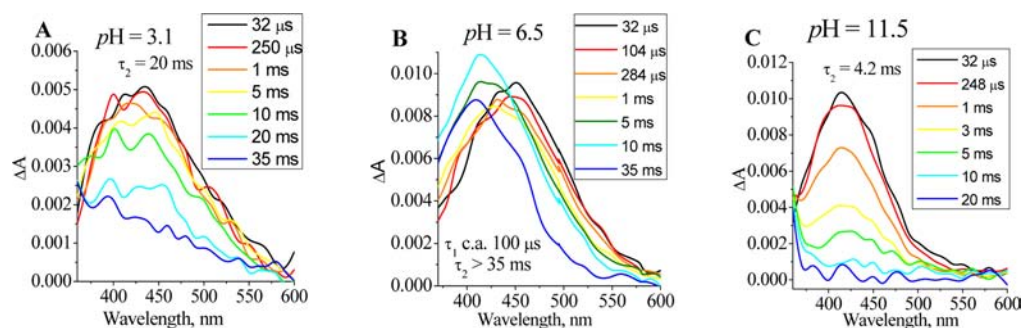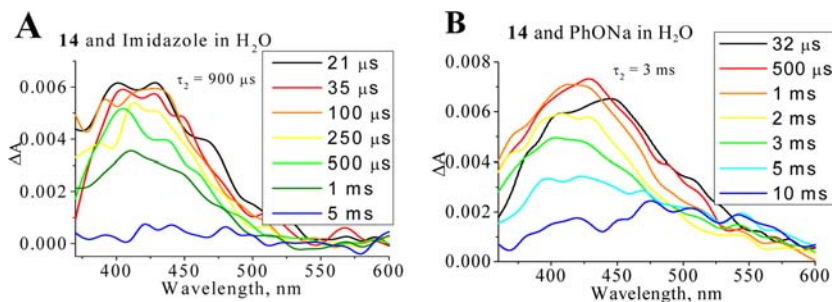

Figure 3. Ultrafast transient absorption spectra of azide **14**. Column A: **14**, 1 mM solution in methanol. Column B: **14**, 0.75 mM in 2-propanol. Time delays in picoseconds between pump and probe pluses are given in the legends. The major time constants describing the ΔA evolution shown are τ = 1.5 ps (A) and τ = 2.5 ps (B).

Table 4. Time Constants τ_1 and τ_2 for the Reactions of Purine Intermediates 15, 23H, and 26 under Various Conditions

Structure	Conditions	Time Constants (τ_1 and τ_2)
15	Aq. $pH = 6.5$	τ_1 ca. 100 µs; τ_2 >35 ms
	Aq. $pH = 11.5$	$\tau_2 = 4.2$ ms
	PhONa	$\tau_2 = 3$ ms
	Imidazole	$\tau_2 = 900$ µs
23H	Aq. $pH = 3.1$	$\tau_2 = 20$ ms
26	MeOH	$\tau_2 = 15$ ms
	Imidazole	$\tau_2 = 75$ µs

Figure 4. Nanosecond−millisecond transient absorption spectra of azide **14** in water at different pH values.

Figure 5. Nanosecond−millisecond transient absorption spectra of azide **14** in water in the presence of (A) imidazole (0.1 M) and (B) sodium phenoxide (0.1 M).
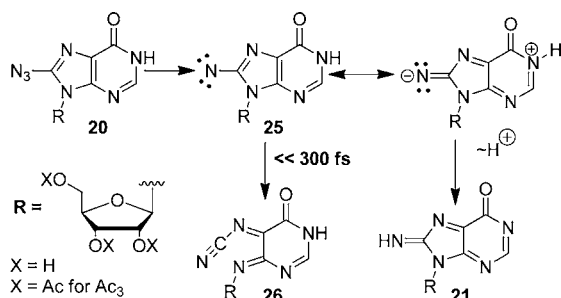
Scheme 14

15
obs λ_{max} = 465 nm
calc λ_{max} = 437nm

24OH
obs λ_{max} = 405 nm

17OH
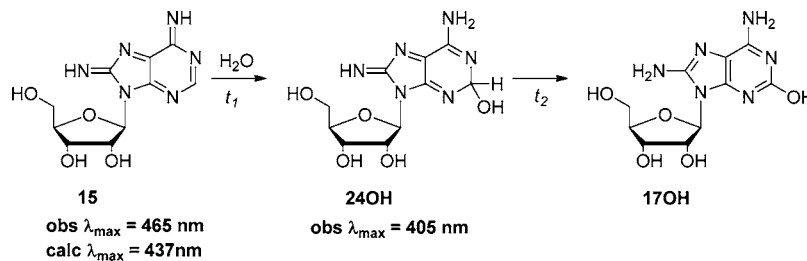
imidazole, $\tau_2 = 75$ µs, than does the diiminoquinone **15**, $\tau_2 =$ 900 µs (Figures 7B and 5A, respectively). It is worthy of note that the absorption associated with the reaction of imidazole with the iminonitrile, **26Ac$_3$**, Figure 7B, derived from **20Ac$_3$** is unusually broad as compared to other transient absorptions

involving reactions of imidazole with iminoquinones **15** and **7** (Figure 5A or 10B, respectively). This extremely broad band may be due to intermediates involved in the ring closure.

Azide **13** is perhaps the most interesting azide studied in this work, because it is a precursor for the natural iminoquinone **7**,
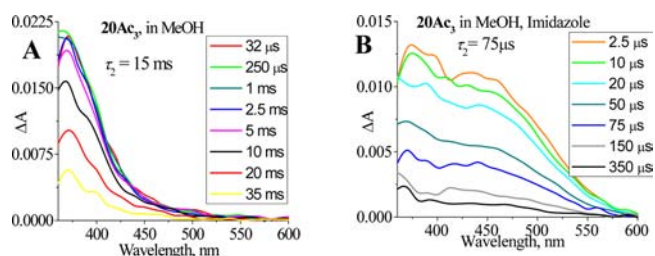
Scheme 15

Figure 7. Microsecond−millisecond transient absorption spectra of azide **20Ac₃** in methanol (A) and in 0.1 M methanolic solution of imidazole (B).

Scheme 16. Ring-opening does not seem to be a viable reaction pathway for nitrene **27**. Instead, nitrene **27** is stabilized via proton reallocation. There are at least two possible mechanisms for proton reallocation as outlined in Scheme 16. The first of these is a direct 1,4-proton shift, and the second is a proton reallocation mediated by a water or an alcohol molecule. The nitrene **27** is expected to be of a similar basicity as nitrene **25**, and therefore not be particularly susceptible to protonation. Consequently, the opening of the six-membered ring of nitrene **27** must be quite slow, if it occurs at all, for the slow proton reallocation to compete effectively. In fact, protonation seems to be the only nitrene stabilization process active in this system. When azide **13Bz₃** was photolyzed in alcohol solvents, Figure 8, bands at λ_{max} = 375 and 550−625 nm are initially formed and slowly shift to a new band centered at λ_{max} = 405 nm. In all cases, the broad band in the 550−625 nm region decays with the same time constant as the growth of the 405 nm band. Therefore, the 375 and 550−625 nm bands have been assigned to the nitrene **27Bz₃** and the 405 nm band assigned to the iminoquinone **7Bz₃** (Scheme 16 and Table 5). In methanol, the proton reallocation time constant is τ = 90 ps and in 2-propanol τ = 300 ps. These observations indicate that the solvent plays an active role in proton reallocation, and therefore the direct 1,4-proton shift mechanism probably is not the only route for the formation of the iminoquinone **7**. This more rapid alcohol-

mediated route is further supported by femtosecond/picosecond flash photolysis data for azide **13Bz₃** in aprotic solvents, Figure 9, in which the strong iminoquinone band of **7Bz₃** at λ_{max} = 405 nm is not observed. In both methylcyclohexane and dichloromethane, **13Bz₃** affords bands at λ_{max} = 345−350 nm and a broad band in the 550−625 nm region. In dichloromethane, the short wavelength band tends to slowly shift to the red to form a new band at ca. 400 nm with a time constant of τ = 600 ps (Figure 9B), while the long wavelength band at 500−650 nm remains stable. These observations are consistent with the calculated absorption spectrum for **27** in Table 5. The short wavelength band centered at λ_{max} = 345−350 nm in methylcyclohexane is assigned to an initially formed singlet nitrene **27s**, which is stable for at least 1 ns, Figure 9A. The same short-time band is observed in dichloromethane, but a new band slowly grows with λ_{max} = 410 nm, τ = 600 ps, Figure 9B.

The broad absorption in the region 550−625 nm changes little, indicating that these changes might be associated with ISC from the singlet nitrene to the triplet nitrene **27t** (λ_{max} = 546 nm). This spectral evolution also might be interpreted as due to formation of both iminoquinone **7** (λ_{max} = 405 nm) produced by the unimolecular proton shift pathway in Scheme 16 and the triplet nitrene **27t** via ISC. Triplet nitrenes such as **27t** would be expected to react via abstraction of hydrogen
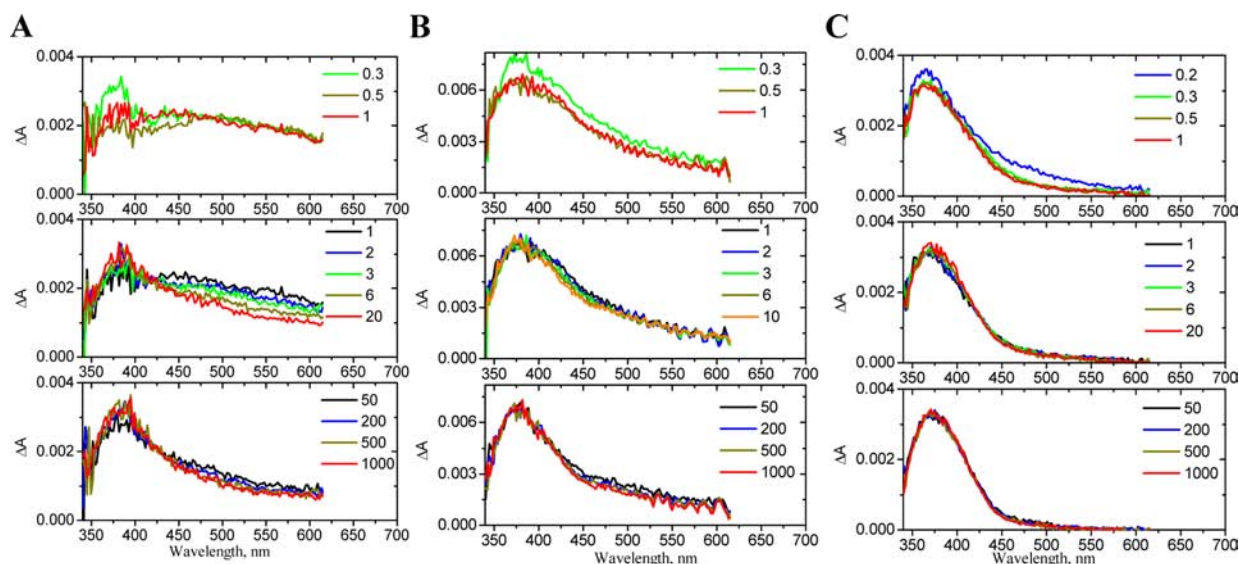

Figure 6. Ultrafast transient absorption spectra of azide **20** (2 mM) solutions in water at pH = 7.5, τ = 7 ps (nitrene **25** decay at 450−600 nm and iminonitrile **26** growth at 380 nm) (A), methanol, τ < 300 fs (nitrene **25** formation and opening to iminonitrile **26**) (B), and **20Ac₃** in dichloromethane, τ < 300 fs (nitrene **25Ac₃** formation and opening to iminonitrile **26Ac₃**) (C). Time delays in picoseconds between pump and probe pluses are given in the legends.
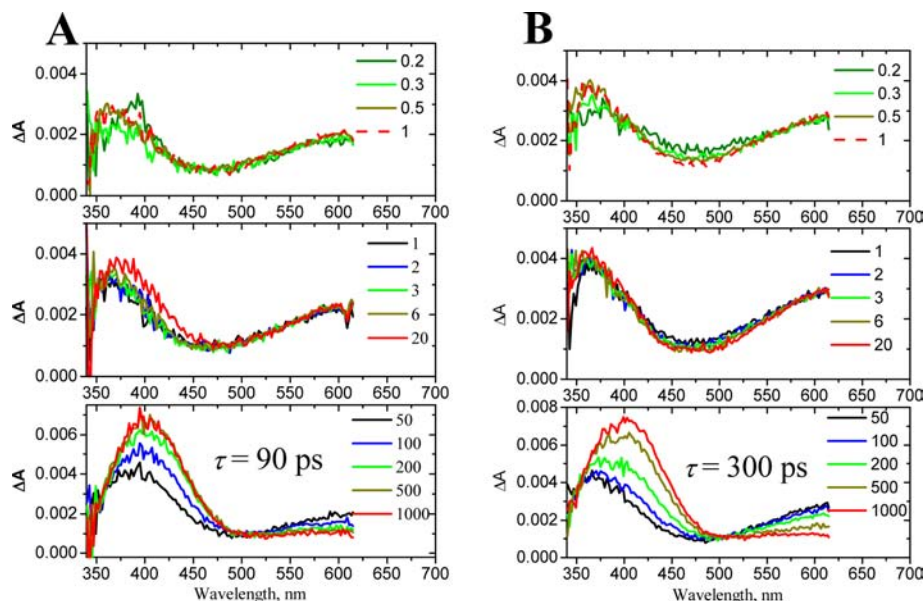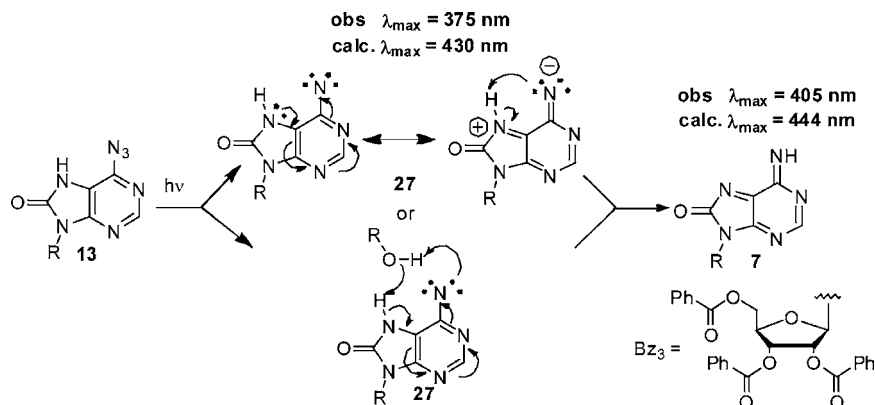
Scheme 16

Figure 8. Ultrafast transient absorption spectra of azide **13Bz$_3$** in MeOH, τ = 90 ps (singlet nitrene **27s** decay at 375 nm and 550−625 nm, and iminoquinone **7Bz$_3$** formation at 405 nm) (A) and in 2-PrOH, τ = 300 ps (singlet nitrene **27s** decay at 375 nm and 550−625 nm, and iminoquinone **7Bz$_3$** formation at 405 nm) (B). Time delays between pump and probe pluses are given in picoseconds in the legends.
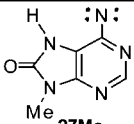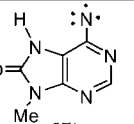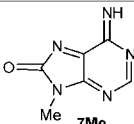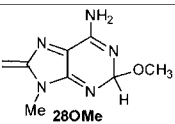
atoms forming the radical **29**, which in turn would ultimately undergo conversion to amine **2** that was isolated from preparative reaction of azide **13Bz$_3$**, Schemes 5 and 17.

The microsecond−millisecond transient absorption spectra for azide **13Bz$_3$** are shown in methanol (Figure 10A) and in 0.1 M solution of imidazole in methanol (Figure 10B). Iminoquinone **7Bz$_3$** is quenched by methanol with a time constant of τ > 30 ms (Figure 10A). This value is slower than that observed for iminonitrile **26Ac$_3$**, τ = 15 ms (Figure 7A). On the other hand, **7Bz$_3$** is quenched by imidazole with a time constant of τ = 20 μs (Figure 10B), which is the fastest of the iminoquinone reactions studied in this work. This adduct formation is associated with a broad adduct band with λ_{max} = 390 nm (Figure 10B and Scheme 17, **28NUC**), but which displays less broadening than the imidazole adduct bands of other systems, Figures 5A and 7B.

Finally, in light of the tendency of guanine to undergo oxidative attack by nucleophiles at the 5-purine ring position, the exclusive attack of adenine-related systems at the 2-position may be surprising. In no case was attack at the 5-position observed in this work. However, in some cases the reaction mixtures were quite complex, and adducts in the 5-position

could have been among the unidentified products; see Table 2. In fact, it is to be expected that nucleophile attack at the 2-position would be the preferred mode of reaction for unsubstituted purines, because this chemistry parallels that previously observed for azide **14**.[26] In addition, the protonation of the nitrenes generated from these purine azides closely parallels the behavior of phenyl nitrenes that are activated by electron-donating substituents.[32] Apparently oxidative addition of nucleophiles to the purine ring only occurs at the 5-position when the 2-position is blocked by prior substitution as in the case of guanosine. Therefore, once the 2-positions of 8-oxoA (**2**) and 8-oxoI (**3**) become substituted, further oxidation should parallel the well-studied 8-oxoG (**1**) pathway.[25] We did not observe guanidinohydantioin, **4**, or spiroiminodihydantion, **5**, Schemes 1 and 18, but the terminal oxidation products, *N* 1′-ribosyl urea, **6**, from the oxidation of **2**, Scheme 2, and the 1-ribosyl guanidine, **18**, from the photoreaction of **14**, Scheme 7, are often observed. Verification of the mechanisms for these advanced stages of purine oxidation will require the development of photochemical methodologies for accessing the 8-oxoG quinone system **9NH$_2$**. The development of these photochemical tools is currently being investigated.

Table 5. Calculated B3LYP/6-31G(d) Vertical Excitation Energies and Oscillator Strengths (f) for Intermediates 27Me, 27t, 7Me, 28OMe, and 28IM[a]

Species	λ (nm) experiment	λ (nm) (f)
27Me Closed-shell Singlet	375 (MeOH) 345-350 (methylcyclohexane or dichloromethane)	430 (0.1509)
27t Triplet	410 (dichloromethane)	546 (0.0496)
7Me	405	444 (0.1096)
28OMe	390	359 (0.0555)
28IM	410	378 (0.0780)

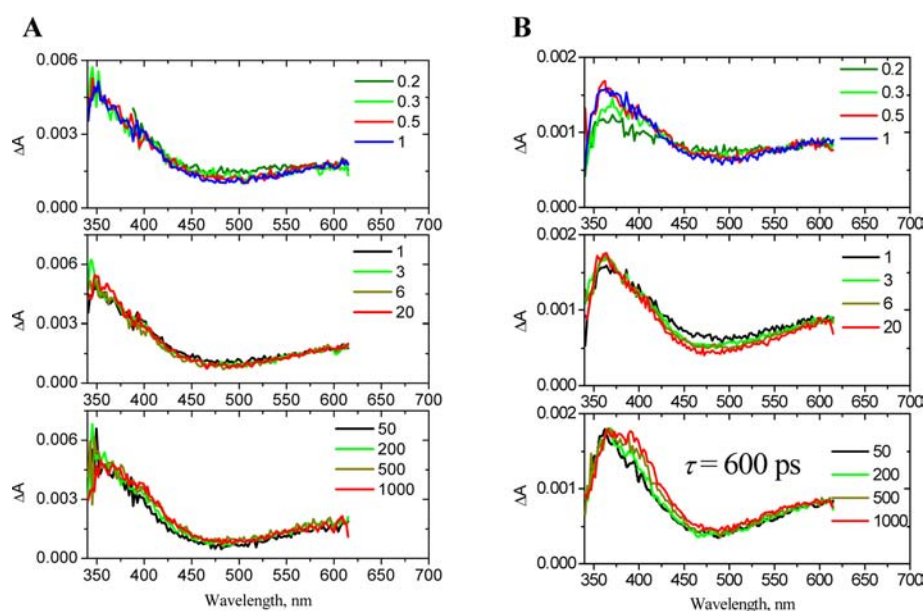[a]All calculations were performed in the gas phase.

Figure 9. Ultrafast transient absorption spectra of azide **13Bz$_3$** in methylcyclohexane (A) and in dichloromethane (B). Time delays in picoseconds between pump and probe pluses are given in the legends. In (B), following the spectral narrowing and reshaping process on a time scale of several picoseconds, the spectral evolution displays a $\tau = 600$ ps rise component.

■ CONCLUSIONS

A working hypothesis for the oxidation of purines was outlined in Scheme 1 and is refined in Scheme 18. The initial oxidation steps to form the 8-oxo-7,8-dihydropurines **1**, **2**, and **3** are well established and have been observed in many biological systems.[1,2] Burrows and Adam have invoked the quinoidal guanosine **9NH$_2$** to explain the further oxidation of **1**,[27−31] and the intermediacy of the related diiminoquinonone **15** has been established in the photochemistry of purine azide **14**.[26] In this work, we have focused upon the possible role of the purine
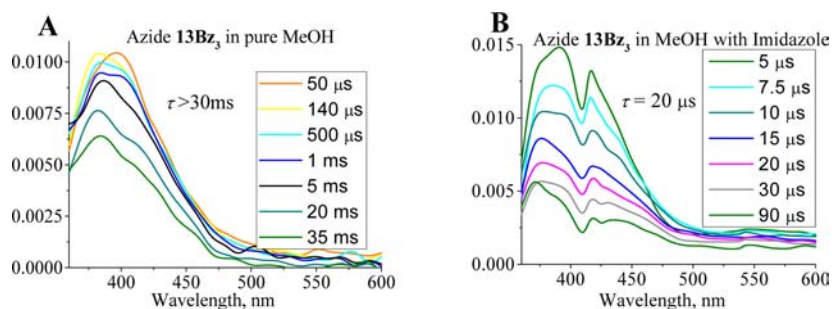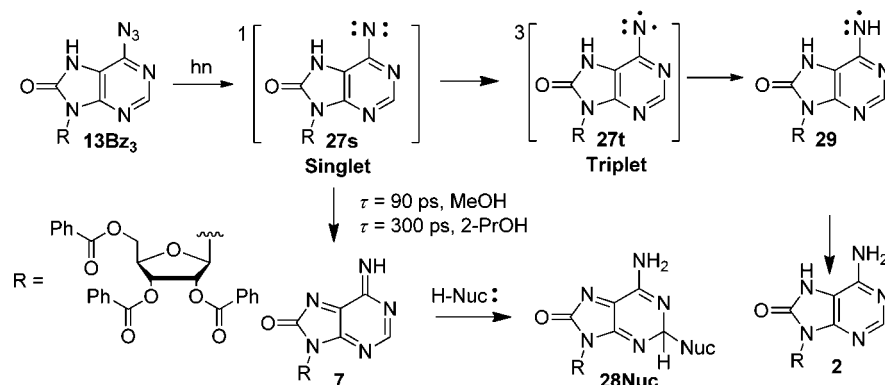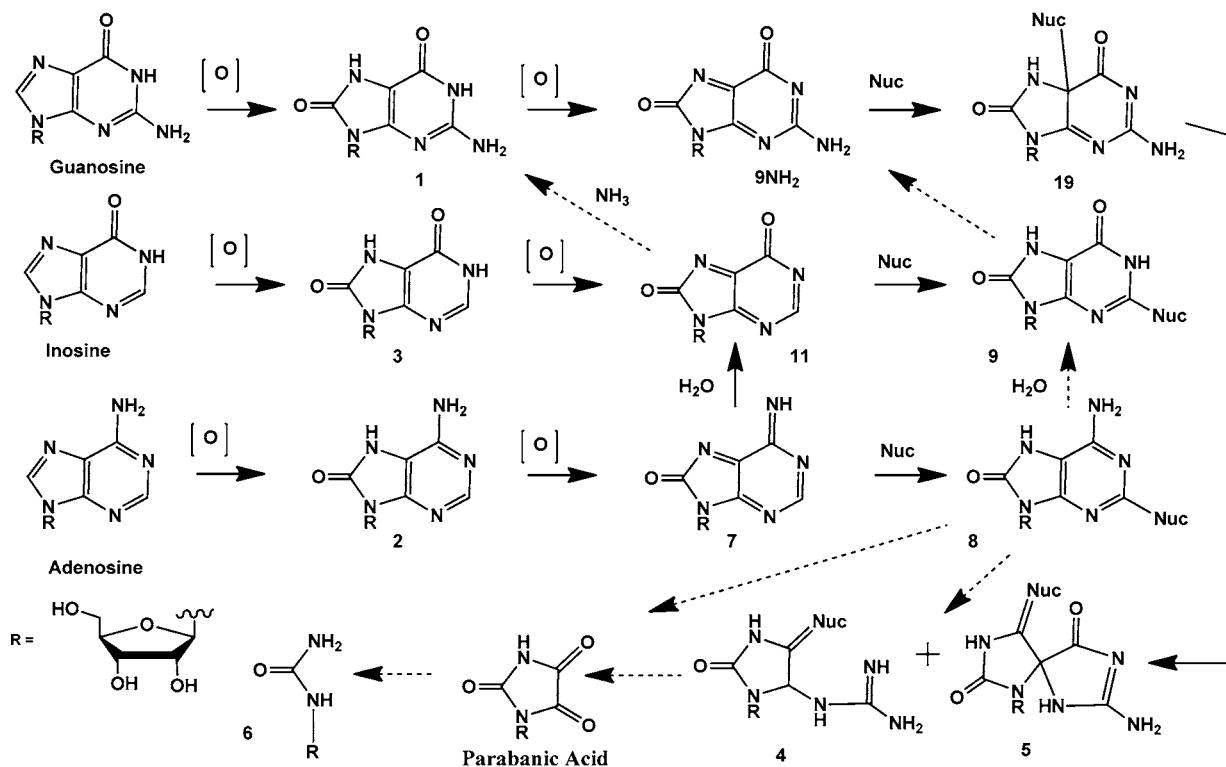
Scheme 17

Figure 10. Microsecond−millisecond transient absorption spectra of azide **13Bz₃** in pure methanol, **28OMe** (A), and in 1 M solution of imidazole in methanol, **28IM** (B).

Scheme 18

iminoquinone **7** and quinone **11** in the oxidation of adenosine and inosine, respectively. The observation of oxidative nucleophilic addition to the 2-position of **2** and **3** in the presence of imidazole supports the intermediacy of **7** and **11**, and the general hypothesis outlined in Scheme 18.

Furthermore, the intermediacy of **7** and its conversion to **8** has been examined in detail using femtosecond and nanosecond transient absorption spectroscopy. These observations strongly support the involvement of the iminoquinone **7** in the further oxidation of **2**. Because **2** is derived from the oxidation

of adenosine (E_{ox} = 1.42 V/NHE), and has been widely observed in biological systems, one can assume that the further oxidation of **2** to **7** (E_{ox} = 0.92 V/NHE) can proceed in living systems as well, and might lead to a wide variety of cross-linking processes in biological systems.

The literature has focused upon the further oxidation of 8-oxo-7,8-dihydroguanosine (**1**) because it is more easily formed than 8-oxo-7,8-dihydroadenosine (**2**). In fact, it has been estimated that the formation of about 10^5 oxidative lesions related to **1** and **2** are formed and repaired each day in the average rat cell.[59] Furthermore, because the ratio of **1**/**2** is about 3/1,[21] the oxidation of adenosine might possibly be of equal or greater significance than that of guanosine. The relative significance of these two types of oxidative lesions might well be biased by the fact that the adenosine lesions tend to form much more stable, less readily repaired, cross-links than do guanosine lesions.

The observation that imidazole forms especially stable adducts with oxidized adenosine deserves comment. The amino acid histidine occurs in the active sites of numerous enzymes, many of which interact with DNA.[60,61] Two particularly interesting cases are His-365 found in the active site of *Escherichia coli* DNA topoisomerase I[62] and the seryl-histidine unit found in the active sites of many hydrolytic enzymes such as the intein−extein junctions of homing endonucleases such as DNAase I.[63] The interaction of these enzymes that function in the routine maintenance of DNA with oxidatively damaged DNA would seem to be a most interesting area for future investigation.

While the work described in this Article significantly extends our understanding of purine oxidation pathways by establishing the viability of quinoidal purine intermediates, it does not address the questions of bridges between the various purine families and the latter stages of purine oxidation to urea **6** and parabanic acid[64,65] shown as dashed arrows in Scheme 18. Further work will be required to elucidate the possible oxidative pathways between **11** and **1**, **8** and **9**, and the ultimate N 1′-ribosyl urea **6**.

Finally, the azide **14** is one of the most widely used photoaffinity labeling agents. The observations reported here further support the intermediacy of the diiminoquinone **15** as the pivotal intermediate in this chemistry.[26] Furthermore, comparison of the transient absorption spectroscopy of **14** with that of **13** is consistent with previously studied nitrene chemistry where it was observed that singlet nitrenes in electronic communication with electron-donating groups become powerful bases and protonate rapidly.[32] Thus, in this work, the activated basic nitrene **22** can be protonated within the first 300 fs, while the deactivated nitrene **27** requires 90−300 ps (Figure 8) for protonation. On the other hand, once protonated, iminoquinone **7** is a more powerful electrophile than the diiminoquinone **15**, and thus might well be a more effective cross-linking agent and PAL agent in many biological systems. Work is continuing to further characterize the chemical reactivity of iminoquinone **7** in duplex nucleic acid environments.

ASSOCIATED CONTENT

Ⓢ Supporting Information

Catalog of chemical structures with their structure numbers, and a description of the instrumentation used to obtain ultrafast femto- and picosecond data. Syntheses of starting materials and characterization of synthetic intermediates, starting materials, and photoproducts. This material is available free of charge via the Internet at http://pubs.acs.org.

AUTHOR INFORMATION

Corresponding Author

atarnov@bgsu.edu; rmw@bgsu.edu

Notes

The authors declare no competing financial interest.

REFERENCES

(1) Wang, D.; Kreutzer, D. A.; Essigmann, J. M. *Mutat. Res.* **1998**, *400*, 99−115.
(2) Cadet, J.; Douki, T.; Gasparutto, D.; Ravanat, J.-L. *Mutat. Res.* **2003**, *531*, 5−23.
(3) Barnes, D. E.; Lindahl, T. *Annu. Rev. Genet.* **2004**, *38*, 445−476.
(4) Nakabeppu, Y.; Sakumi, K.; Sakamoto, K.; Tsuchimoto, D.; Tsuzuki, T.; Nakatsu, Y. *Biol. Chem.* **2006**, *387*, 373−379.
(5) Wilson, D. M.; Bohr, V. A. *DNA Repair* **2007**, *6*, 544−559.
(6) Finkel, T.; Holbrook, N. J. *Nature* **2000**, *408*, 239−247.
(7) Feig, D. I.; Loeb, L. A. *J. Mol. Biol.* **1994**, *235*, 33−41.
(8) Wiseman, H.; Halliwell, B. *Biochem. J.* **1996**, *313*, 17−29.
(9) Steenken, S.; Jovanovic, S. V. *J. Am. Chem. Soc.* **1997**, *119*, 617−618.
(10) Solivio, M. J.; Joy, T. J.; Sallans, L.; Merino, E. J. *J. Inorg. Biochem.* **2010**, *104*, 1000−1005.
(11) Solivio, M. J.; Nemera, D. B.; Sallans, L.; Merino, E. J. *Chem. Res. Technol.* **2012**, *25*, 326−336.
(12) Tan, X.; Grollman, A. P.; Shibutani, S. *Carcinogenesis* **1999**, *20*, 2287−2292.
(13) von Sonntag, C. *Free-Radical-Induced DNA Damage and Its Repair: A Chemical Perspective*; Springer-Verlag: New York, 2006; pp 211−447.
(14) Bjelland, S.; Seeberg, E. *Mutat. Res.* **2003**, *531*, 37−80.
(15) Dirks, A. J.; Hofer, T.; Marzetti, E.; Pahor, M.; Leeuwenburgh, C. *Aging Res. Rev.* **2006**, *5*, 179−195.
(16) Hofer, T.; Seo, A. Y.; Prudencio, M.; Leeuwenburgh, C. *Biol. Chem.* **2006**, *387*, 103−111.
(17) Hofer, T.; Badouard, C.; Bajak, E.; Ravanat, J.-L.; Mattsson, A.; Cotgreave, I. A. *Biol. Chem.* **2005**, *386*, 333−337.
(18) Dizdaroglu, M. *Mutat. Res.* **2003**, *531*, 109−126.
(19) Michaels, M. L.; Tchou, J.; Grollman, A. P.; Miller, J. H. *Biochemistry* **1992**, *31*, 10964−10968.
(20) Jaruga, P.; Dizdaroglu, M. *Nucleic Acids Res.* **1996**, *24*, 1389−1394.
(21) Llano, J.; Eriksson, L. A. *Phys. Chem. Chem. Phys.* **2004**, *6*, 4707−4713.
(22) Ito, T.; Kuno, S.; Uchida, T.; Fujita, J.-i.; Nishimoto, S.-i. *J. Phys. Chem. B* **2009**, *113*, 389−394.
(23) Jensen, A.; Calvayrac, G.; Karahalil, B.; Bohr, V. A.; Stevnsner, T. *J. Biol. Chem.* **2003**, *278*, 19541−19548.
(24) Grin, I. R.; Dianov, G. L.; Zharkov, D. O. *FEBS Lett.* **2010**, *584*, 1553−1557.

(25) Perrier, S.; Hau, J.; Gasparutto, D.; Cadet, J.; Favier, A.; Ravanat, J.-L. *J. Am. Chem. Soc.* **2006**, *128*, 5703−5710.

(26) Polshakov, D.; Rai, S.; Wilson, R. M.; Mack, E. T.; Vogel, M.; Krause, J. A.; Burdzinski, G.; Platz, M. S. *Biochemistry* **2005**, *44*, 11241−11253.

(27) Xu, X.; Fleming, A. M.; Muller, J. G.; Burrows, C. J. *J. Am. Chem. Soc.* **2008**, *130*, 10080−10081.

(28) Johansen, M. E.; Muller, J. G.; Xu, X.; Burrows, C. J. *Biochemistry* **2005**, *44*, 5660−5671.

(29) Hosford, M. E.; Muller, J. G.; Burrows, C. J. *J. Am. Chem. Soc.* **2004**, *126*, 9540−9541.

(30) Ye, Y.; Muller, J. G.; Luo, W.; Mayne, C. L.; Shallop, A. J.; Jones, R. A.; Burrows, C. J. *J. Am. Chem. Soc.* **2003**, *125*, 13926−13927.

(31) Adam, W.; Arnold, M. A.; Nau, W. M.; Pischel, U.; Saha-Möller, C. R. *J. Am. Chem. Soc.* **2002**, *124*, 3893−3904.

(32) Voskresenska, V.; Wilson, R. M.; Panov, M.; Tarnovsky, A. N.; Krause, J. A.; Vyas, S.; Winter, A. H.; Hadad, C. M. *J. Am. Chem. Soc.* **2009**, *131*, 11535−11547.

(33) Mack, E. T. University of Cincinnati, unpublished results.

(34) Yanagawa, H.; Ogawa, Y.; Ueno, M. *J. Biol. Chem.* **1992**, *267*, 13320−13326.

(35) Steenken, S.; Jovanovic, S. V.; Bietti, M.; Bernhard, K. *J. Am. Chem. Soc.* **2000**, *122*, 2373−2374.

(36) Adam, W.; Saha-Möller, C. R.; Schönberger, A.; Berger, M.; Cadet, J. *J. Photochem. Photobiol.* **1995**, *62*, 231−238.

(37) Sheu, C.; Foote, C. S. *J. Am. Chem. Soc.* **1995**, *117*, 474−477.

(38) Sheu, C.; Foote, C. S. *J. Am. Chem. Soc.* **1995**, *117*, 6439−6442.

(39) Raoul, S.; Cadet, J. *J. Am. Chem. Soc.* **1996**, *118*, 1892−1898.

(40) Adam, W.; Saha-Möller, C. R.; Schönberger, A. *J. Am. Chem. Soc.* **1996**, *118*, 9233−9238.

(41) Duarte, V.; Gasparutto, D.; Yamaguchi, L. F.; Ravanat, J.-L.; Martinez, G. R.; Medeiros, M. H. G.; Di Mascio, P.; Cadet, J. *J. Am. Chem. Soc.* **2000**, *122*, 12622−12628.

(42) Luo, W.; Muller, J. G.; Rachlin, E. M.; Burrows, C. J. *Chem. Res. Toxicol.* **2001**, *14*, 927−938.

(43) Duarte, V.; Muller, J. G.; Burrows, C. J. *Nucleic Acids Res.* **1999**, *27*, 496−502.

(44) Luo, W.; Muller, J. G.; Rachlin, E. M.; Burrows, C. J. *Org. Lett.* **2000**, *2*, 613−616.

(45) Temple, C., Jr.; Montgomery, J. A. *J. Org. Chem.* **1965**, *30*, 826−829.

(46) Temple, C., Jr.; Coburn, W. C., Jr.; Thorpe, M. C.; Montgomery, J. A. *J. Org. Chem.* **1965**, *30*, 2395−2398.

(47) Temple, C., Jr.; Thorpe, M. C.; Corburn, W. C., Jr.; Montgomery, J. A. *J. Org. Chem.* **1966**, *31*, 935−938.

(48) Addicott, C.; Wong, M. W.; Wentrup, C. *J. Org. Chem.* **2002**, *67*, 8538−8546.

(49) Marburg, S.; Jorn, D.; Tolman, R. L. *J. Heterocycl. Chem.* **1982**, *19*, 671−672.

(50) Gadosy, T. A.; McClelland, R. A. *J. Am. Chem. Soc.* **1999**, *121*, 1459−1465.

(51) Dehaen, W.; Becher, J. *Acta Chem. Scand.* **1993**, *47*, 244−254.

(52) Funicello, M.; Spagnolo, P.; Zanirato, P. *Acta Chem. Scand.* **1993**, *47*, 231−243.

(53) Spinelli, D.; Zanirato, P. *J. Chem. Soc., Perkin Trans. 2* **1993**, 1129−1133.

(54) Assignment of spectral bands was supported by theoretical calculations using Gaussian 09 and MOLCAS 7.4 software: (a) Frisch, M. J.; Trucks, G. W.; Schlegel, H. B.; Scuseria, G. E.; Robb, M. A.; Cheeseman, J. R.; Scalmani, G.; Barone, V.; Mennucci, B.; Petersson, G. A.; Nakatsuji, H.; Caricato, M.; Li, X.; Hratchian, H. P.; Izmaylov, A. F.; Bloino, J.; Zheng, G.; Sonnenberg, J. L.; Hada, M.; Ehara, M.; Toyota, K.; Fukuda, R.; Hasegawa, J.; Ishida, M.; Nakajima, T.; Honda, Y.; Kitao, O.; Nakai, H.; Vreven, T.; Montgomery, J. A., Jr.; Peralta, J. E.; Ogliaro, F.; Bearpark, M.; Heyd, J. J.; Brothers, E.; Kudin, K. N.; Staroverov, V. N.; Kobayashi, R.; Normand, J.; Raghavachari, K.; Rendell, A.; Burant, J. C.; Iyengar, S. S.; Tomasi, J.; Cossi, M.; Rega, N.; Millam, N. J.; Klene, M.; Knox, J. E.; Cross, J. B.; Bakken, V.; Adamo, C.; Jaramillo, J.; Gomperts, R.; Stratmann, R. E.; Yazyev, O.; Austin, A. J.; Cammi, R.; Pomelli, C.; Ochterski, J. W.; Martin, R. L.; Morokuma, K.; Zakrzewski, V. G.; Voth, G. A.; Salvador, P.; Dannenberg, J. J.; Dapprich, S.; Daniels, A. D.; Farkas, Ö.; Foresman, J. B.; Ortiz, J. V.; Cioslowski, J.; Fox, D. J. *Gaussian 09*, revision A.1; Gaussian, Inc.: Wallingford, CT, 2009. (b) MOLCAS 7.4: Aquilante, F.; De Vico, L.; Ferré, N.; Ghigo, G.; Malmqvist, P.; Neogrády, P.; Pedersen, T. B.; Pitoňák, M.; Reiher, M.; Roos, B. O.; Serrano-Andrés, L.; Urban, M.; Veryazov, V.; Lindh, R. *J. Comput. Chem.* **2010**, *31*, 224−247.

(55) Peon, J.; Polshakov, D.; Kohler, B. *J. Am. Chem. Soc.* **2002**, *124*, 6428−6438.

(56) Dix, E. J.; Goodman, J. L. *J. Phys. Chem.* **1994**, *98*, 12609−12612.

(57) Pines, E.; Pines, D.; Barak, T.; Magnes, B. Z.; Tolbert, L. M.; Haubrich, J. E. *Ber. Bunsen-Ges.* **1998**, *102*, 511−517.

(58) Lima, J. C.; Abreu, I.; Brouillard, R.; Macanita, A. L. *Chem. Phys. Lett.* **1998**, *298*, 189−195.

(59) Park, E.-M.; Shigenaga, M. K.; Degan, P.; Korn, T. S.; Kitzler, J. W.; Wehr, C. M.; Kolachana, P.; Ames, B. N. *Proc. Natl. Acad. Sci. U.S.A.* **1992**, *89*, 3375−3379.

(60) Luscombe, N. M.; Laskowski, R. A.; Thornton, J. M. *Nucleic Acids Res.* **2001**, *29*, 2860−2874.

(61) Leavens, F. M. V.; Churchill, C. D. M.; Wang, S.; Wetmore, S. D. *J. Phys. Chem. B* **2011**, *115*, 10990−11003.

(62) Perry, K.; Mondragón, A. *J. Biol. Chem.* **2002**, *277*, 13237−13245.

(63) Li, Y.; Hatfield, S.; Li, J.; McMills, M.; Zhao, Y.; Chen, X. *Bioorg. Med. Chem.* **2002**, *10*, 667−673.

(64) Vialas, C.; Claparols, C.; Pratviel, G.; Meunier, B. *J. Am. Chem. Soc.* **2000**, *122*, 2157−2167.

(65) Jena, N. R.; Mishra, P. C. *Free Radical Biol. Med.* **2012**, *53*, 81−94.